Available online at www.sciencedirect.com
SCIENCE DIRECT
Carbohydrate Polymers 65 (2006) 253–262
Carbohydrate Polymers
www.elsevier.com/locate/carbpol

Differential scanning calorimetry and dielectric properties of methyl-2-hydroxyethyl cellulose doped with erbium nitrate salt

Gamal Sobhai Said [a,*], Fawazy Hamed Abd-El Kader [b], Mohamed Mahross El Naggar [a], Badawi Ali Anees [a]

[a] *Solid State Physics, Fayoum University, Faculty of Science Physics Department, Fayoum, Egypt*
[b] *Experimental Physics, Cairo University, Faculty of Science, Giza, Egypt*

Received 20 November 2005; received in revised form 6 January 2006; accepted 10 January 2006
Available online 24 February 2006

Abstract

Cast technique was used to prepare thin films of pure methyl-2-hydroxyethyl cellulose (MHEC) and composite samples containing erbium trinitrate [$Er(NO_3)_3$] films with concentrations 0.5, 1, 2, 5, 7, and 10 wt%. Differential scanning calorimetry (DSC) was performed on pure materials [MHEC and $Er(NO_3)_3$] and their composites of 2 and 10 wt% $Er(NO_3)_3$. The new exothermic phase transitions induced in DSC thermograms may be attributed to structural phase transitions. The dielectric constant (ε'), dielectric loss (ε''), and ac-conductivity σ_{ac} were studied for MHEC and $Er(NO_3)_3$ doped MHEC samples as a function of temperature and frequency. The activation energies for both α and σ-relaxation processes observed in ε' and ε'' for the samples under investigation were calculated. It was found that the value of activation energy calculated for of σ-relaxation process is consistent with that of dc-conductivity for all doped samples in the same temperature range. In addition, the correlated barrier hopping mechanism of the electrons appeared to be the most suitable mechanism to describe the ac conduction behavior in different compositions of the present system.

Keywords: Methyl-2-hydroxyethyl cellulose; $Er(NO_3)_3$; Dielectric properties; Correlated barrier hopping; Relaxation processes

1. Introduction

One of the goals of material research is to create and develop new materials tailored to a particular application and to understand the physical mechanisms that determine their properties. Depending on the chemical nature of the doping substance and the way in which they interact with the host matrix, the dopant alters the physical properties to different degrees (El-Shekeil, Al-Moydama, Al-Karbooly, & Khalid, 1999).

DSC is capable of providing information about the crystalline phase and the transition temperature. It is particularly useful in studying the crystallinity of the samples to provide direct measurements of thermodynamical properties such as heat of fusion and melting point.

One of the methods to characterize materials is based on the analysis of their dielectric spectra. Dielectric analysis provides the information about the motion of entities having an electric charge or an electric dipole moment, i.e., dipole reorientation, rotations of the main and segmental chains and conductivity mechanisms (Liedermann & Lapcik, 2000). In the present work, a systematic investigation has been made on the characteristics of the phase transitions and the dielectric properties of MHEC doped with erbium nitrate. Both frequency and temperature will be varied for dielectric measurements, so that a wide range of molecular mobility can be examined.

2. Experimental details

Methyl-2-hydroxyethyl cellulose was supplied by Sigma–Aldrich Company, USA, with a viscosity of approximately 15,000–20,000 cp. Hydrated erbium trinitrate was

* Corresponding author. Tel.: +2 02 8374170.
E-mail address: badawi_sc@yahoo.com (G.S. Said).

0144-8617/$ - see front matter © 2006 Elsevier Ltd. All rights reserved.
doi:10.1016/j.carbpol.2006.01.009

supplied by Strem Chemicals Company, USA, with purity 99.9%. The solution method was employed to obtain film samples. Weighted amounts of MHEC and $Er(NO_3)_3$ were dissolved in tridistilled water and in pure nitric acid at room temperature, respectively. Solutions of MHEC and $Er(NO_3)_3$ were mixed together with different weight percentages (0.5, 1, 2, 5, 7, and 10 wt%), the mixture was mechanically stirred by using a magnetic stirrer at 30 °C. Thin films of appropriate thickness (~120 μm) were cast onto a glass petri dish of 10 cm diameter, and then dried in an oven at about 70 °C for about 3 days until the solvent was completely evaporated. Films were cut into square pieces of side 1 cm.

Thermal analysis was carried out using a computerized differential scanning calorimetry (DSC), $T_{A\text{-}50}$ Schimadza Corporation, Kyoto, Japan. Measurements were carried out under nitrogen atmosphere (30 ml/min). The heating rate used for all samples under investigation is 10 °C/min. Measurements of the dielectric constant ε' and dielectric loss ε'' in the frequency range 1 kHz to 1 MHz and a controlled temperature range from 30 to 180 °C were carried out using (Hioki 3532 Hitester Programmable RLC meter). The ac electrical conductivity σ_{ac} of the sample is taken as $\sigma_{ac} = \omega\ \varepsilon_0\varepsilon''$. The dc-conductivity measurements were also conducted using an electrometer (Keithely 6517A).

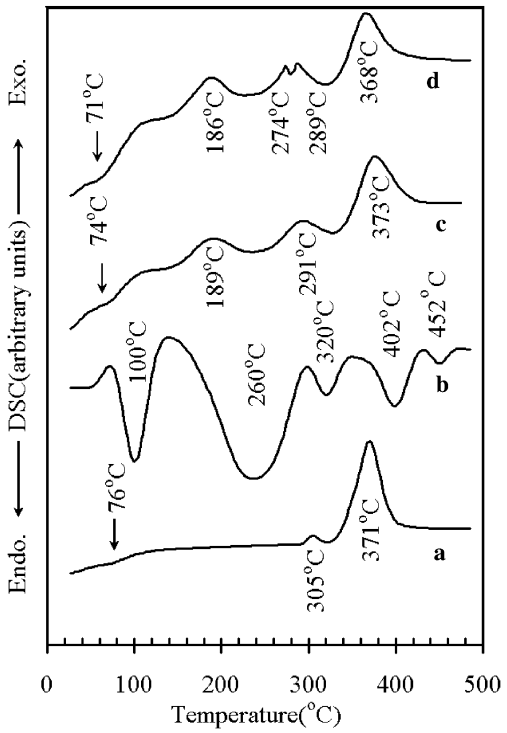

Fig. 1. DSC thermograms for (a) MHEC, (b) $Er(NO_3)_3$, (c) 2 wt% $Er(NO_3)_3$, and (d) 10 wt% $Er(NO_3)_3$.

3. Results and discussion

3.1. Differential scanning calorimetry

The presence of water as a solvent could modify self-association of MHEC and also interaction between components in the composite samples. This material is heat-sensitive; after thermal treatment their absorption capacity for the water is modified. Therefore, the films under investigation were annealed at 100 °C for 20 min for complete evaporation of water solvent before any studies.

Fig. 1a shows the DSC thermogram for pure MHEC in the temperature range from 30 up to 500 °C. Three phase transitions appeared at 76, 305, and 371 °C associated with enthalpies 93.20, 8.30, and 320.00 J/g, respectively. The first shallow and broad endothermic phase transition may correspond to the glass transition temperature (T_g). The broad glass transition is apparently a result of the nonuniform nature of this process. The two last exothermic successive phase transitions are attributed to some sort of structural modification, evolution and/or decomposition of MHEC. Since there is not any reported T_g value for MHEC, the obtained T_g value from DSC measurement is compared with the previously reported for 2-hydroxyethyl cellulose (HEC). It must be noted that the T_g value for MHEC is higher than HEC (62 °C) (Marianiava, Lapcik, & Pisarcik, 1992). Thus, it can be suggested that the extra CH_3 group presents in MHEC than HEC is associated with increased intermolecular interaction such as an increase in crosslink density and entanglement. In addition, the melting phase transition for MHEC could not be observed in the measured temperature range of the DSC scan. This may be a direct result of the rigid rod nature of MHEC molecular backbones making them susceptible to degradation before melting. This phenomenon is in fact typical for many other polysaccharides (Peesan, Rujiravanit, & Supaphol, 2003).

The DSC for erbium trinitrate hydrates $Er(NO_3)_3{\cdot}6H_2O$ in powder form is shown in Fig. 1b. Five endothermic phase transitions have appeared at about 100, 260, 320, 402, and 452 °C associated with enthalpies of 185, 510, 110, 180, and 50 J/g, respectively. It is known (Landt & Bear, 1960) that erbium trinitrate loses four molecules of water at about 130 °C, so the first endotherm was due to the fusion of the erbium nitrate hydrates. This was followed by gradual dehydration reactions which took place over a 240–280 °C temperature range (Strydom & Van Vuuren, 1988). Because of these gradual dehydration reactions, the endotherm appeared as a broad peak. Before the dehydration was completed, the erbium nitrate began to decompose through a series of oxynitrate as shown by the next three small endotherms. The terminal product in the oxynitrates decomposition was the erbium oxide. The erbium trinitrate melts beyond 500 °C which is out of the programmed temperature range of DSC scan.

It was of particular interest to estimate how the thermal transition of MHEC varied after mixing with different concentrations of erbium trinitrate. DSC thermograms of MHEC doped with concentrations 2 and 10 wt% $Er(NO_3)_3$ samples are illustrated in Figs. 1c and d. It is clear that the position of T_g for MHEC films doped with different amounts of $Er(NO_3)_3$ was slightly shifted towards lower

temperatures than pure MHEC (≈75 °C). This indicates that the segmental mobility of amorphous MHEC increases with the addition of $Er(NO_3)_3$. The most important feature of these thermograms is the appearance of one additional exothermic peak for 2 wt% $Er(NO_3)_3$ at 189 °C while for 10 wt% $Er(NO_3)_3$ another additional exothermic peak appeared at 274 °C other than ordinary as presented of MHEC. Therefore, the appearance of these exothermic phase transitions may be attributed to some sort of structural modification induced due to the addition of $Er(NO_3)_3$. Thus, it may be concluded that there are some specific intermolecular interactions between both metal and nitrate ions with the host matrix of MHEC.

3.2. Dielectric properties

3.2.1. Dielectric constant

Fig. 2 represents the temperature dependence of dielectric constant (ε') for MHEC in the frequency range from 1 kHz to 1 MHz. It can be seen that each $\varepsilon'(T)$ curve contains only one pronounced broad relaxation peak centered at about 70 °C with a magnitude of 17 at 1 kHz. It must be noticed that there is a quantitative difference observed for the position of T_g in DSC (≈75 °C) and the dielectric analysis (≈70 °C). This deviation may be attributed to the different "levels of structure" detected by different techniques and scanning rates, in addition to the instruments employed.

As shown from Fig. 2 the dielectric constant decreases with increasing the frequency over the whole investigated range of temperature. At glass transition temperature, ε' varies from 17 to 9 for a frequency range from 1 kHz to 1 MHz. With increasing frequency the behavior is identical except that the peak position slightly changes toward progressively higher temperatures. The shift in peak position is in the range 69–74 °C for the frequency range 1 kHz–1 MHz. The general variation of $\varepsilon'(T)$ for MHEC is in conformity with that previously reported in literature (El-Shahawy & El-Kholy, 1994; Marianiava et al., 1992). for many polar polymers. The increase of ε' with temperature up to T_g is governed mainly by the change in the intra- and inter-molecular interactions. These interactions may involve the alignment or rotation of the dipoles present in the polymer with the increase of temperature. Above T_g, the dielectric constant begins to fall due to the increase in the chaotic thermal oscillation of the molecules and the diminishing degree of order of the orientation of the dipoles (Sharma & Ramu, 1991).

Fig. 3 shows the temperature dependence of dielectric constant for MHEC composite samples containing 0.5, 1, 2, 5, 7, and 10 wt% $Er(NO_3)_3$ at 1 kHz. The dielectric constant analysis of the composite samples yields two broad peaks, one occurs within the glass transition region of MHEC and the other at a higher temperature at about 165 °C. The higher temperature peak is related to the doping of $Er(NO_3)_3$ to polymer matrix.

It is noticed that the values of ε' for various MHEC/$Er(NO_3)_3$ composite samples is higher than in pure MHEC sample over the whole temperature range. Among these samples, the value of ε' for the composite sample of 2 wt% $Er(NO_3)_3$ content is the highest one. The inset of Fig. 3 shows that the values of dielectric constant of the peak maximum (ε'_{max}) at the glass transition. The values

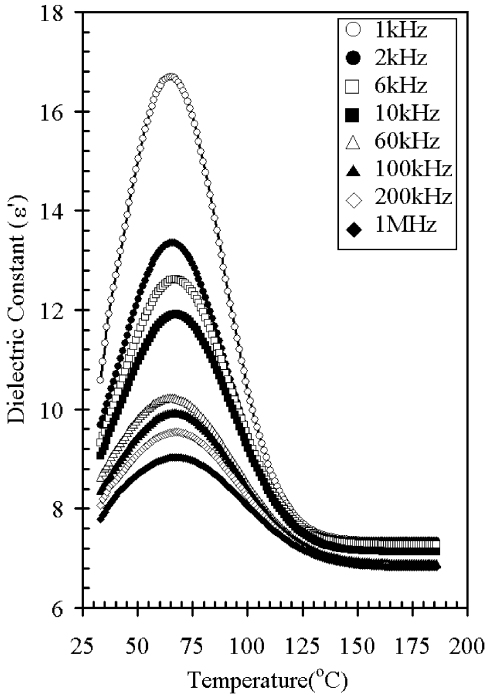

Fig. 2. Temperature dependence of ε' for pure MHEC at different frequencies.

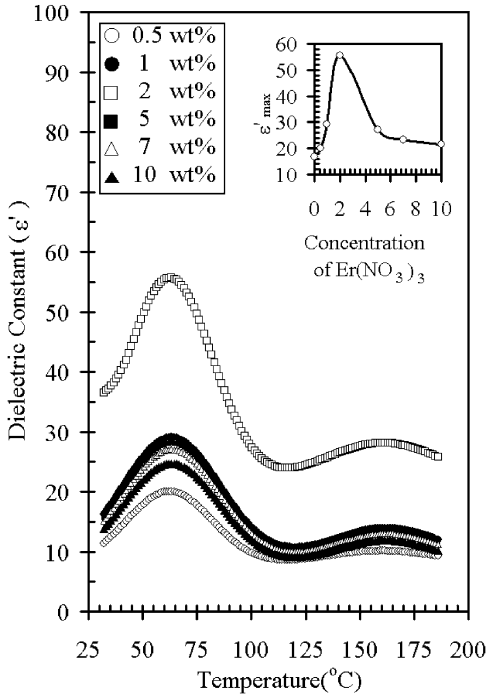

Fig. 3. Temperature dependence of ε' for MHEC–$Er(NO_3)_3$ composites samples at 1 kHz.

increase with increasing dopant content up to 2 wt% and then decreases with increasing dopant up to 10 wt%. At low dopant concentration of $Er(NO_3)_3$ ($\leqslant$2 wt%), the complex formation is facilitated and the number of ionizable charge carriers increases considerably in the polymer network, so the ε' will increase. While at higher percentage of $Er(NO_3)_3$ (>2 wt%) the solubility limit of dopant is reached and may partially act as an intermolecular plasticizer where $Er(NO_3)_3$ molecules are distributed in the inter-aggregate space. This will hinder the polymer chain elongation and consequently results in the decrease of ε'.

Dielectric properties are usually related to the permanent or induced dipoles in the polymeric chains or to space charge effects which are found in composite materials. Classically the relation of the dielectric constant, ε', to the permanent dipole, μ_0, is given by

$$\frac{\varepsilon'-1}{\varepsilon'+2}=\frac{4\pi N}{3}\left[(\alpha_e+\alpha_i)+\frac{\mu_0^2}{3kT}\right], \quad (1)$$

where α_e and α_i are the electronic and ionic polarizability, respectively, μ_0 is the dipole moment in Debye, N is the number of molecules per unit volume, k is Boltzmann's constant, and T is the absolute temperature. The slope of straight line (Fig. not shown) of the relation between $\frac{\varepsilon'-1}{\varepsilon'+2}$ and $\frac{1}{T}$ above the glass transition temperature of the different samples is related to the square of the dipole moment. The calculated dipole moments in Debye units for MHEC, 0.5, 1, 2, 5, 7, and 10 wt% $Er(NO_3)_3$ are 39, 35, 32, 16, 26, 34, and 37 ± 0.5, respectively. It is interesting to note that the values of μ_0 for the composite samples are less than that for the pure MHEC having the lowest value for the composite 2 wt% $Er(NO_3)_3$. This behavior can be attributed to the decrease in chain space and the free volume between dipoles as well as the increase in the degree of ordering of dipole orientation due to mixing $Er(NO_3)_3$ with MHEC.

Fig. 4 shows the behavior of dielectric constant ε' of 2 wt% $Er(NO_3)_3$ as a representative of the all samples in the frequency range from 1 kHz to 1 MHz at some selected temperatures 40, 50, 60, 70, 100, 120, and 140 °C. It must be noticed that the change in ε' is significant at low frequencies for all the samples. The decrease in dielectric constant with frequency for the investigated samples at a given temperature may be attributed mainly to the decreasing number of dipoles which contribute to polarization. It is worth noting that ε' tends to lower values at higher frequencies, which may be ascribed to the space charge polarization and interfacial polarization as a result of the defects and heterogeneity present in polymer matrix. In addition, the magnitude of dielectric dispersion with increasing frequency depends on temperature which becomes largely noticeable as the temperature increased towards the glass transition.

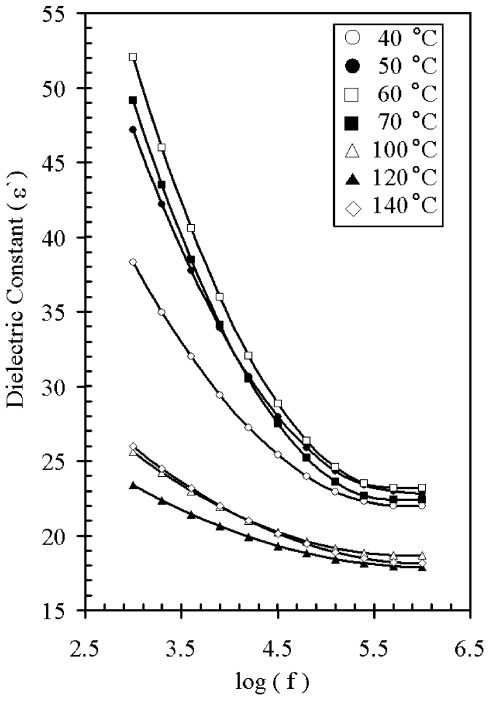

Fig. 4. The variation of ε' with frequency for 2 wt% $Er(NO_3)_3$ at different temperatures.

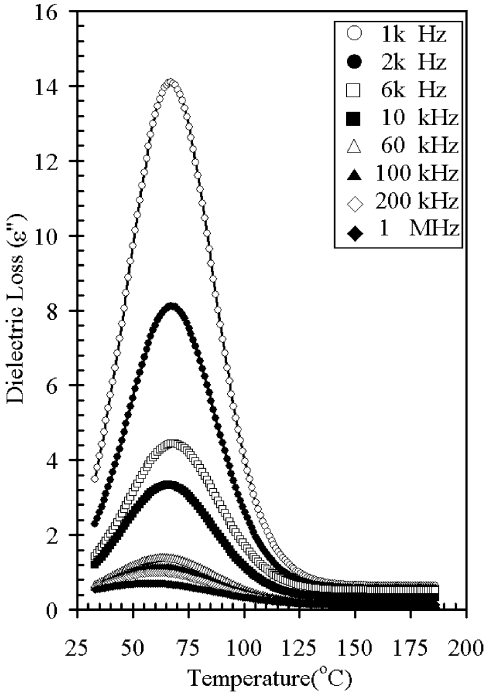

Fig. 5. Temperature dependence of ε'' for pure MHEC at different frequencies.

3.2.2. Dielectric loss factor

Fig. 5 exhibits the temperature dependence of dielectric loss factor ε'' for pure MHEC in the frequency range from 1 kHz to 1 MHz. Only one relaxation peak is observed in the region of glass transition on each $\varepsilon''(T)$ curve. It is peak position shifted towards higher temperature with increasing frequency. This relaxation is attributed to micro-Brownian motion of large chain segments. Which is a semi-cooperative action involving torsional oscillation and/or rotation about the backbone bonds in a given chain

as well as in neighboring chains. The relaxation peak corresponding to the glass transition in MHEC may be explained using the free volume theory (Fox & Flory, 1948). Accordingly, the molecular mobility (and consequently, the relaxation time) near T_g mainly depends on the free volume. In the glassy state, the free volume will be frozen and will remain at a constant value; the whole size and distribution of the free volume within the glass will similarly remain fixed below T_g. The glass will, however, expand with increasing temperature due to normal expansion process of all molecules, which result from the changing vibrational amplitudes of bond distances (Roberts & White, 1973). About T_g, in addition to the normal expansion process, there will be an expansion of free volume itself, which will result in a large expansion of the rubber like polymer. This yields a sufficient place for molecular motion by rotation or translation to occur. Due to this increase in chain segment mobility, there will be a large increase in the loss factor (ε'') at T_g (Rellick & Rund, 1986).

Fig. 6 shows the temperature dependence of dielectric loss factor (ε'') at 1 kHz for 0.5, 1, 2, 5, 7, and 10 wt% $Er(NO_3)_3$ doped MHEC samples. Two relaxation peaks are noticed. The first relaxation peak corresponding to the glass transition (α-relaxation), while the higher temperature relaxation peak may be assigned to ions migration in the disordered structure of the polysaccharide material (Einfeldt, Meißner, & Kwasniewski, 2001; Huang, 2003).

For natural and synthetic polymers it is common to distinguish between the primary (α-relaxation), which is related to the glass transition temperature T_g, and several secondary relaxations. Some of the latter are observed in the sub-T_g range are related either to the local main chain dynamic (β-relaxation), to side-group motion (γ-relaxation) or to an orientational motion of associated groups (clusters) of molecules. It was found recently (El-Shafee & Saad, 1993; Mudarra et al., 2001) that an additional dielectric relaxation process called σ-relaxation process, could be observed in the high temperature range (80–180 °C) for amorphous solid systems and polysaccharides. This σ-relaxation process has been associated with the hopping motion of ions in the disordered structure of the polymer material which is strongly related to the dc-conductivity of the polymer system. A similar process has been observed for many years from the work of Taylor (1956), Stevels (1980), and Yamamoto and Namikawa (1988) in ionic conducting disordered solids such as glasses and ceramics.

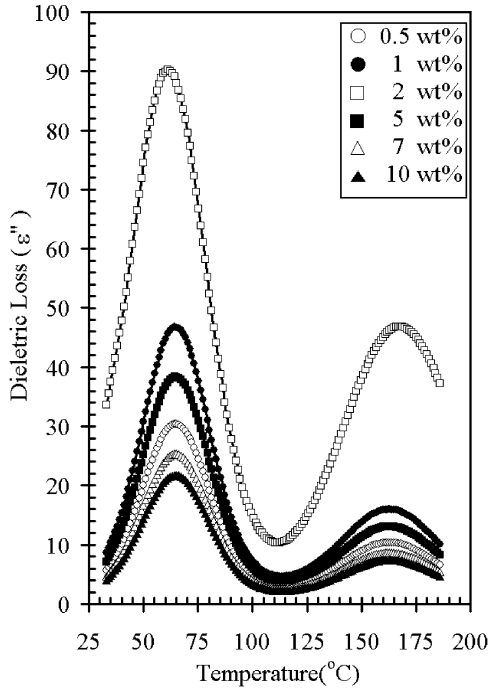

Fig. 6. Temperature dependence of ε'' for MHEC–$Er(NO_3)_3$ composites samples at 1 kHz.

The main argument for the physical connection of both dielectric and dc-conductivity processes is that the values of the activation energies for both processes are nearly equal. Although the α- and σ-relaxation processes are broad, since they are related to the distribution of the relaxation times and/or activation energies, Debye type treatment, assuming a single relaxation process will be employed (Hill, Vaughan, Price, & Davies, 1969; El-Sayed & Fayek, 2005).

The real and imaginary parts of complex permittivity ε' and ε'' are given by:

$$\varepsilon' = \varepsilon_\infty + \frac{\varepsilon_s - \varepsilon_\infty}{1 + \omega^2\tau^2}, \tag{2}$$

$$\varepsilon'' = (\varepsilon_s - \varepsilon_\infty)\frac{\omega\tau}{1 + \omega^2\tau^2}, \tag{3}$$

by solving both Eqs. (2) and (3), the following relation is obtained:

$$\log\left(\frac{\varepsilon''}{\omega}\right) = \log(\varepsilon' - \varepsilon_\infty) + \log\tau. \tag{4}$$

The plots of $\log(\varepsilon''/\omega)$ vs $\log(\varepsilon' - \varepsilon'_\infty)$ at some temperature points which correspond to the lower temperature side of both (α- and σ-relaxation processes) for pure and doped MHEC containing 0.5, 1, 2, 5, 7, and 10 wt% $Er(NO_3)_3$ show the same behavior. Accordingly, Figs. 7a and b are given here for NHEC and 2 wt% $Er(NO_3)_3$ as representatives for the all series. The value of dielectric constant at 1 MHz was taken to be ε'_∞. Applying linear fitting for these data, the values of relaxation time (τ) have been deduced and are listed in Table 1.

The values of the calculated τ for both α- and σ-relaxation processes are in the order (10^{-7}–10^{-13} s) and (10^{-5}–10^{-12} s), respectively, depending on both temperature and dopant concentrations. The smaller values of relaxation time $\tau = 10^{-13}$ s in α-relaxation process for 2 wt% $Er(NO_3)_3$ composite sample is indicative of the cooperative character of the molecular motion in this transition and that the dipoles have an excess freedom of motion.

The temperature dependence of the relaxation time $\tau(T)$ is represented in the form of an Arrhenius relation:

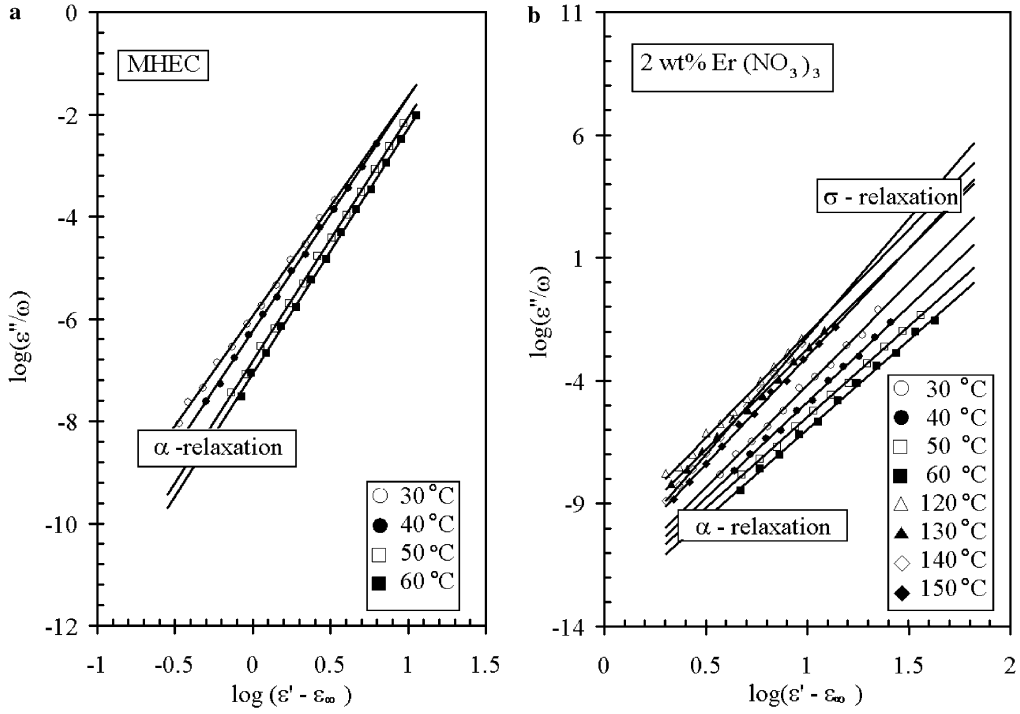

Fig. 7. The Debye relation for (a) pure MHEC and (b) 2 wt% $Er(NO_3)_3$ for both (α- and σ-relaxations).

Table 1
The values of relaxation time τ (s) for MHEC and $Er(NO_3)_3$ doped MHEC for α- and σ-relaxations

MHEC/$Er(NO_3)_3$ (wt/wt)%	100/0.0	99.5/0.5	99/1	98/2	95/5	93/7	90/10
30 °C	7.95×10^{-7}	2.13×10^{-9}	3.35×10^{-12}	1.77×10^{-13}	2.18×10^{-10}	3.45×10^{-8}	2.15×10^{-10}
40 °C	3.98×10^{-7}	1.59×10^{-9}	2.20×10^{-12}	2.00×10^{-13}	1.20×10^{-10}	1.85×10^{-8}	1.11×10^{-10}
50 °C	1.30×10^{-7}	9.93×10^{-10}	1.84×10^{-12}	1.50×10^{-13}	8.55×10^{-11}	9.50×10^{-9}	9.00×10^{-11}
60 °C	9.60×10^{-8}	8.51×10^{-10}	1.25×10^{-12}	9.00×10^{-14}	5.88×10^{-11}	6.30×10^{-9}	5.95×10^{-11}
120 °C	–	4.80×10^{-6}	1.95×10^{-8}	5.40×10^{-12}	3.65×10^{-7}	2.81×10^{-5}	4.20×10^{-7}
130 °C	–	3.40×10^{-6}	1.30×10^{-8}	4.15×10^{-12}	2.20×10^{-7}	1.77×10^{-5}	2.60×10^{-7}
140 °C	–	2.45×10^{-6}	1.00×10^{-8}	3.45×10^{-12}	1.50×10^{-7}	1.14×10^{-5}	1.30×10^{-7}
150 °C	–	1.60×10^{-6}	5.37×10^{-9}	2.32×10^{-12}	9.00×10^{-8}	6.10×10^{-6}	9.55×10^{-8}

$$\tau(T) = \tau_0 \exp(E_a/kT), \tag{5}$$

where E_a is the activation energy of the relaxation process and τ_0 is the pre-exponential factor. The data were fitted to a straight line whose slope is the activation energy parameter for the relaxation processes in the investigated samples. The calculated values of the activation energy for both α- and σ-processes in all samples are presented in Table 2. It is noticed that the activation energy of α-relaxation is lower than the activation energy values for σ-relaxation in all composite samples which may be due to the increase of chain separation and free volume which facilitates dipolar orientation that mainly contributes to polarization. Whereas the relaxation activation energy values for σ-process is influenced by the specific mean distances between high potential barriers for the ion migration or geometrical dimensions of the conducting pathways.

In Fig. 8 the temperature dependence of the dc-conductivity is shown in the form of an activation plot at the high temperature range for pure and doped samples. All samples have evidently shown an Arrhenius behavior of the form

$$\sigma(T) = \sigma_0 \exp(-E_{dc}/kT). \tag{6}$$

From the slope of theses curves the activation energies of the electrical conductivity E_{dc} were calculated (see Table 2).

Comparing the Arrhenius plots of the temperature dependence of the conductivity of Fig. 8 and the relaxation time of the σ-relaxation process for all $Er(NO_3)_3$ doped MHEC samples, the two processes yield nearly the same activation energy varying between 0.65 and 0.90 eV for all substances.

Fig. 9 shows the correlation between the dc-conductivity in the form of a double logarithmic plot, which represents a migration property of movable ions, and the relaxation time of the σ-process, which corresponds with the formation of dipolar structures in the material. For all composite samples examined, the points are located on a straight line for each substance showing an excellent correlation

Table 2
The values of activation energies for (α- and σ-relaxations) and dc-conductivity for pure MHEC and doped samples with $Er(NO_3)_3$

MHEC/$Er(NO_3)_3$ (wt/wt)%	α-relaxation E_α (eV)	σ-relaxation E_σ (eV)	E_{dc} (eV)	$B = E_\sigma/E_{dc}$	A
100/0.0	0.40	–	0.92	–	–
99.5/0.5	0.38	0.82	0.85	0.97	−17.59
99/1	0.33	0.70	0.73	0.95	−18.58
98/2	0.28	0.68	0.65	1.05	−20.95
95/5	0.35	0.78	0.74	1.07	−20.43
93/7	0.36	0.82	0.81	1.00	−17.50
90/10	0.38	0.89	0.85	1.06	−21.00

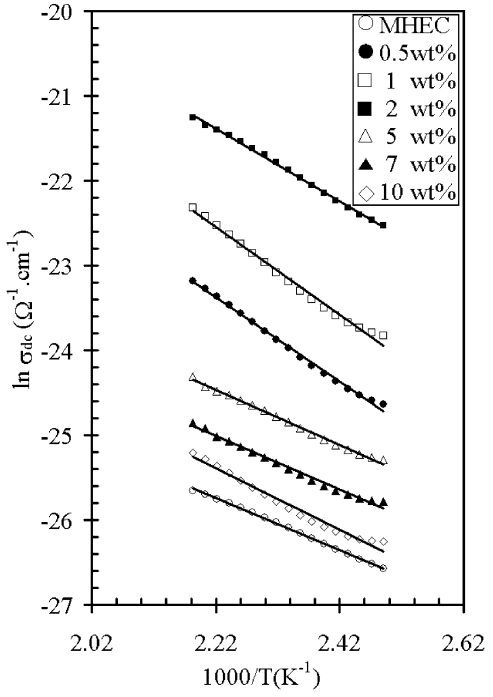

Fig. 8. Activation energy plots of the dc-conductivity for pure MHEC and MHEC–$Er(NO_3)_3$ composites samples.

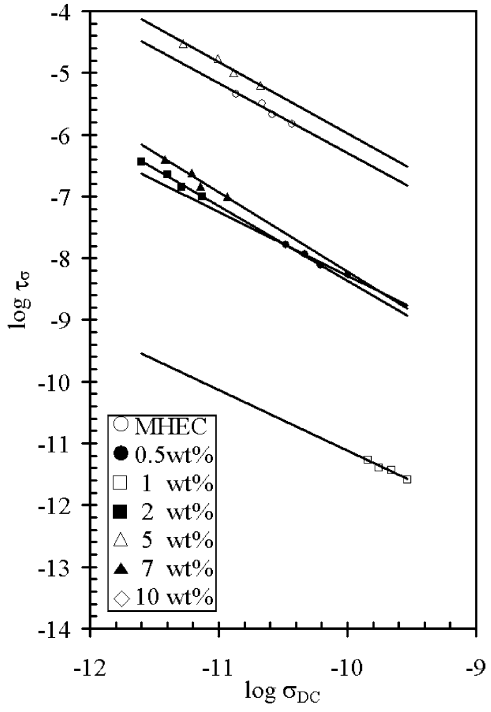

Fig. 9. The relation between $\log \tau_\sigma$ and $\log \sigma_{DC}$ for MHEC–$Er(NO_3)_3$ composites samples.

between both quantities. This relation can be expressed by the following relationship:

$$\log \tau_\sigma = A + B \log \sigma_{dc}, \quad (7)$$

which can be easily deduced from Eqs. (5) and (6). B is the fraction of both activation energies: $B = E_\sigma/E_{dc}$ covering values between 0.97 and 1.06 for all samples examined. The relation between both τ_σ and σ_{dc} quantities which are physically completely different processes shows correlation coefficients, which were higher than 0.97 in all cases. Thus, it can be concluded that there is a strong correlation between the relaxation time of σ-relaxation and the dc-conductivity.

3.3. ac-conductivity

In general the ac-conductivity of the amorphous materials, where the charge carriers experience an approximately random energy on diffusing, is found to obey $\sigma(\omega) = A\omega^s$, where the exponent $s \leqslant 1$ (up to 1 MHz) (Padmasree & Kanchan, 2005; Rao, Raghavaiah, Rao, & Veeraiah, 2005), and considered to signify the coupling of ions movement with its environment (Austin & Mott, 1969; Nagai, 1979). A careful temperature-dependent study of the exponent frequency s is expected to be helpful in elucidating the microscopic dielectric relaxation mechanism responsible for the ac losses.

To determine the dominant ac conduction mechanism which is effective in the present compositions, the dependence of σ_{ac} on the frequency at different temperature points corresponding to the lower temperature side of both α- and σ-relaxations processes was considered. Fig. 10 shows the frequency dependence of $\sigma_{ac}(\omega)$ at temperatures 30, 40, 50, and 60 °C for α-relaxation and temperatures 120, 130, 140, and 150 °C for σ-relaxation, respectively, for 2 wt% $Er(NO_3)_3$ (as a representative). As can be seen, the plots yield straight lines for all considered temperatures. This type of behavior reveals that the exponent s is independent of frequency; hence the mechanism responsible for ac conduction could be a hopping one. It is found

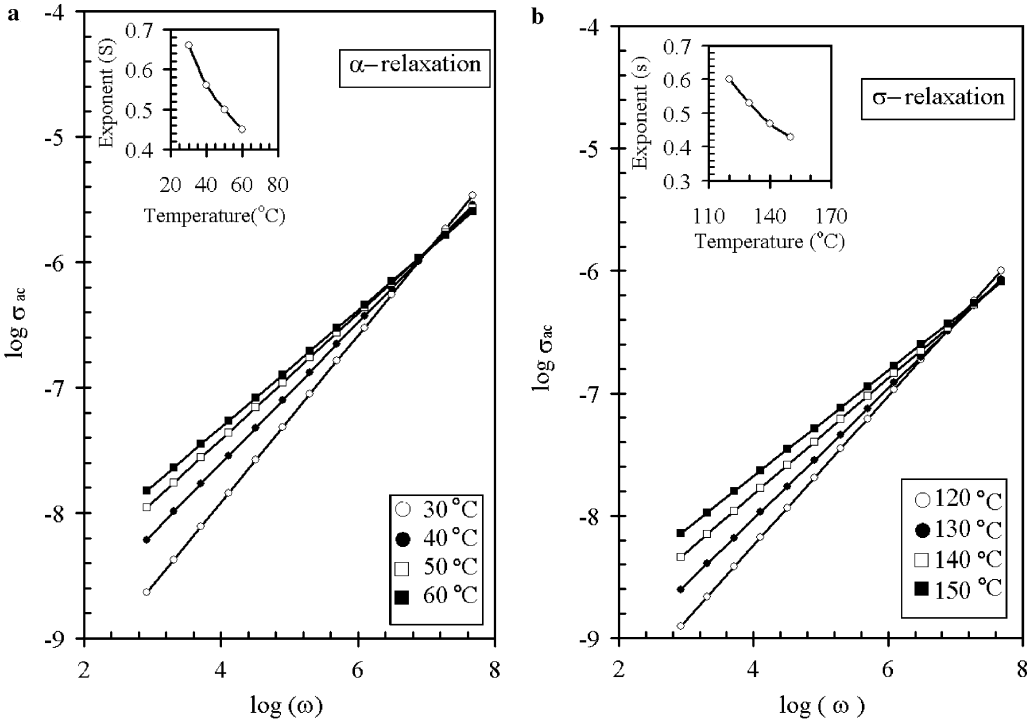

Fig. 10. The relation between $\log(\sigma)$ and $\log(\omega)$ for 2 wt% (a) α-relaxation and (b) σ-relaxation.

to be consistent with that observed in many hopping systems (De, De, Das, & De, 2005; Papaioannou, Patermarakis, & Karayianni, 2005; Thamilselvan, Nazeer, Mangalaraj, Narayandass, & Yi, 2004; Wang, Fu, Gopalan, & Wen, 2004). Values of s were derived by calculating the slopes of frequency dependence $\sigma_{ac}(\omega)$. It is observed that the exponent s decreases with increasing temperature (see the inset of Fig. 10) and its values is less than unity, i.e., $0 < s < 1$ for both α and σ relaxations. Accordingly, these results lead to the prediction that the correlated barrier hopping (CBH) is the most suitable mechanism to explain the ac conduction behavior in the investigated materials (Bhatnagar & Bhatida, 1990; Wang et al., 2004).

In this model (Bhatnagar & Bhatida, 1990), the temperature dependence of s follows the equation:

$$s = 1 - \frac{6kT}{U_M - kT\ln(1/\omega\tau_0)}, \tag{8}$$

where U_M is the maximum barrier height at infinite separation, which is called the polaron binding energy, i.e., the binding energy of the carrier in its localized sites, τ_0 is a characteristic relaxation time which is in the order of an atomic vibrational period ($\approx 10^{-13}$ s). For neighboring sites at a separation R, the coulomb wells overlap, resulting in a lowering in of the effective barrier from U_M to value of U_h, which for the case of a single electron transition, is given by

$$U_h = U_M - \frac{e^2}{4\pi\varepsilon_0\varepsilon' R}, \tag{9}$$

where the hopping distance R at a given frequency ω is given by

$$R_\omega = \frac{e^2}{\pi\varepsilon_0\varepsilon'[U_M - kT\ln(1/\omega\tau)]}. \tag{10}$$

For large values of U_M/kT the exponent s becomes

$$s = 1 - \frac{6kT}{U_M}. \tag{11}$$

And the lower bound (cut-off) to hopping distance R_{min} is given by

$$R_{min} = \frac{e^2}{\pi\varepsilon_0\varepsilon' U_M}. \tag{12}$$

Using the values of s, the maximum barrier height at infinite separation U_M could be calculated according to Eq. (11) and listed in Table 3 along with other pertinent data. The values of U_M show a decrease with increasing temperature for both α- and σ-relaxations in all investigated samples. The relatively small decrease of U_M by increasing temperature is due to thermal agitation which leads to an increase of the degree of overlap of the coulombic potential wells of the considered sites. Also, it must be noticed that the values of both s and U_M are changed irregularly with the $Er(NO_3)_3$ dopant concentration at all selected temperatures. Comparing the values of U_M obtained from the ac-conductivity with the magnitude of the activation energies E_a (for both α- and σ-relaxation processes) from the relaxation process reported, earlier for pure and composite samples one can easily note that the values of U_M (for σ-relaxation) are relatively lower than that of E_a. This difference in the values indicates the micro-inhomogeneity of the samples under investigation (Bhatnagar & Bhatida, 1990).

Table 3
The ac-parameters for pure MHEC and its composites for both α- and σ-relaxations

MHEC/Er$(NO_3)_3$ (wt/wt)%	100/0.0				99/1.0				98/2.0				95/5.0				90/10			
	R (nm)	R_{min} (nm)	U_h (eV)	U_M (eV)	R (nm)	R_{min} (nm)	U_h (eV)	U_M (eV)	R (nm)	R_{min} (nm)	U_h (eV)	U_M (eV)	R (nm)	R_{min} (nm)	U_h (eV)	U_M (eV)	R (nm)	R_{min} (nm)	U_h (eV)	U_M (eV)
30 °C	1.63	1.40	0.35	0.45	0.95	0.85	0.35	0.46	0.60	0.53	0.36	0.47	1.10	0.93	0.32	0.41	1.15	1.10	0.32	0.40
40 °C	1.58	1.28	0.32	0.40	0.88	0.70	0.30	0.38	0.55	0.43	0.30	0.37	0.88	0.78	0.30	0.39	0.98	0.86	0.30	0.38
50 °C	1.46	1.10	0.30	0.37	0.85	0.60	0.28	0.33	0.50	0.37	0.28	0.34	0.78	0.65	0.29	0.37	0.87	0.72	0.29	0.36
60 °C	1.38	0.95	0.28	0.35	0.80	0.53	0.27	0.32	0.44	0.29	0.27	0.32	0.77	0.60	0.28	0.35	0.85	0.66	0.28	0.35
120 °C	–	–	–	–	2.56	1.05	0.04	0.50	1.23	0.60	0.05	0.52	2.15	1.25	0.04	0.47	2.10	1.35	0.04	0.49
130 °C	–	–	–	–	2.37	1.12	0.39	0.44	0.90	0.50	0.39	0.45	2.00	1.20	0.38	0.44	1.95	1.30	0.36	0.44
140 °C	–	–	–	–	2.25	1.05	0.37	0.42	0.82	0.40	0.36	0.41	1.76	1.15	0.36	0.42	1.90	1.20	0.32	0.39
150 °C	–	–	–	–	1.26	0.58	0.35	0.40	0.73	0.37	0.34	0.39	1.59	1.14	0.35	0.39	1.62	1.12	0.30	0.40

The hopping distance R, the lower bound (cut-off) R_{min} and the Coulomb barrier height U_h are calculated using Eqs. (9)–(12), respectively. It must be remembered that the value of the characteristics relaxation time presented in Table 1 is used in the calculation of R in Eq. (10). The values of the ac-parameters R, R_{min}, and U_h at different temperatures for both α- and σ-relaxations are listed in Table 3 from which it is clear that R, R_{min}, and U_h tend to decrease slightly with increasing temperature for both pure and doped samples for their relative α- and σ-relaxations processes. The results strongly confirm that the correlated barrier hopping mechanism depends on the composition and temperature in the present investigated samples.

4. Conclusions

1. The $\varepsilon'(T)$ and $\varepsilon''(T)$ curves are found to shift slightly towards higher temperatures with increasing the frequency. This well-known feature is a characteristic of the freezing of the dipolar motion with no longer-range correlation (i.e., glass-like).
2. There is a strong correlation between the relaxation time of the σ-relaxation and the dc-conductivity in the same temperature region for all composite samples. The activation energies of both physically different processes were nearly equal. These confirm the concept that ion hopping in the disordered solid system can lead to a relaxation process.
3. The character of dependence of the power s on temperature has revealed that the correlated barrier hopping (CBH) model to be the most dominate mechanism which can contribute to the ac conduction behavior in the tested compositions of the present system.

References

Austin, I. G., & Mott, N. F. (1969). Polarons in crystalline and non-crystalline materials. *Advances in Physics, 18*, 41–102.

Bhatnagar, V. K., & Bhatida, K. L. (1990). Frequency dependent electrical transport in bismuth modified amorphous germanium sulfide semiconductors. *Journal of Non-Crystalline Solids, 119*, 214–231.

De, S., De, A., Das, A., & De, S. K. (2005). Transport and dielectric properties of α-zirconium phosphate-polyaniline composite. *Materials Chemistry and Physics, 91*, 473–477.

Einfeldt, J., Meißner, D., & Kwasniewski, A. (2001). Polymerdynamics of cellulose and other polysaccharides in solid state – secondary dielectric relaxation processes. *Progress in Polymer Science, 26*, 1419–1472.

El-Sayed, S. M., & Fayek, S. A. (2005). Low temperature dielectric behavior and ac conductivity in metal-containing chalcogenide Ge_2S_3 films. *Solid State Ionics, 176*, 149–154.

El-Shafee, E., & Saad, G. R. (1993). Dielectric analysis of poly(vinyl chloride) films doped with cobalt(II) chloride. *Polymer Degradation and Stability, 41*, 25–29.

El-Shahawy, M. A., & El-Kholy, M. M. (1994). Dielectric properties of cobalt-doped poly(vinyl-chloride). *European Polymer Journal, 30*, 259–263.

El-Shekeil, A., Al-Moydama, H., Al-Karbooly, A., & Khalid, M. A. (1999). DC electrical conductivity of poly [4-amino-2,6-pyrimidinodithio carbamate] and its metal complexes. *Polymer, 40*, 2879–2887.

Fox, T. G., & Flory, P. J. (1948). Viscosity–molecular weight and viscosity–temperature relationship for polystyrene and polyisobutylene. *Journal of American Chemical Society, 70*, 2384–2395.

Hill, N., Vaughan, W. E., Price, A. H., & Davies, M. (1969). *Dielectric properties and molecular behavior*. London: Van Nostrand.

Huang, Y. (2003). Thermotropic behavior of hydroxyethyl cellulose acetate. *Journal of Applied Polymer Science, 51*, 1979–1984.

Landt, W. W. W., & Bear, J. L. (1960). Thermal decomposition of the heavier rare earth metal nitrate: Thermobalance and differential thermal analysis studies. *Journal of Inorganic Nuclear Chemistry, 12*, 276–280.

Liedermann, K., & Lapcik, L. Jr, (2000). Dielectric relaxation in hydroxyethyl cellulose. *Carbohydrate Polymers, 42*, 369–374.

Marianiava, D., Lapcik, L., & Pisarcik, M. (1992). Study of the dielectric properties of cellulose derivatives. *Acta Polymerica, 34*, 303–306.

Mudarra, M., Colleja, R. D., Belana, J., Canadas, J. C., Diego, J. A., Sellares, J., & Sanchis, M. J. (2001). Study of space charge relaxation in PMMA at high temperature by dynamic dielectric analysis. *Polymer, 42*, 1647–1651.

Nagai, K. L. (1979). Universality of low-frequency fluctuation, dissipation and relaxation properties of condensed matter. *Comments Solid State Physics, 9*, 127–140.

Padmasree, K. P., & Kanchan, D. K. (2005). Dielectric studies on CdI_2 doped Ag_2O–V_2O_5–B_2O_5 system. *Materials Chemistry and Physics, 91*, 551–557.

Papaioannou, J. C., Patermarakis, G. S., & Karayianni, H. S. (2005). Electron hopping mechanism in hematite (α-Fe_2O_3). *Journal of Physics and Chemistry of Solids, 66*, 839–844.

Peesan, M., Rujiravanit, R., & Supaphol, P. (2003). Characterization of beta-chitin/poly (vinyl alcohol) blends films. *Polymer Testing, 22*, 381–387.

Rao, P. N., Raghavaiah, B. V., Rao, D. K., & Veeraiah, N. (2005). Studies on dielectric properties of LiF–Sb_2O_5–B_2O_5:CuO glass system. *Materials Chemistry and Physics, 91*, 381–390.

Rellick, G. S., & Rund, J. (1986). A dielectric study of poly(ethyelene-co-vinylacetate)-poly(vinyl chloride) blends: Miscibility and phase behavior. *Journal of Polymer Science: Polymer Physics, 24*, 279–302.

Roberts, G. E., & White, E. F. T. (1973). In R. N. Howard (Ed.), *Physics of glassy polymers*. London: Applied Science Publishers.

Sharma, A. K., & Ramu, Ch. (1991). Dielectric properties of solution grown cellulose acetate thin films. *Materials Letters, 11*, 128–132.

Stevels, J. M. (1980). Local motions in ditreous systems. *Journal of Non-Crystalline Solids, 40*, 69–82.

Strydom, C. A., & Van Vuuren, C. P. J. (1988). Some observations on the thermal decomposition kinetics of gadolinium(III), holmium(III) and erbium(III) nitrate. *Thermochimica Acta, 129*, 335–339.

Taylor, H. E. (1956). The dielectric relaxation spectrum of glass. *Transactions of the Faraday Society, 52*, 873–881.

Thamilselvan, M., Nazeer, K. P., Mangalaraj, D., Narayandass, S. K., & Yi, J. (2004). Effect of substrate temperature on ac conduction properties of amorphous and polycrystalline GaSe thin films. *Materials Research Bulletin, 39*, 1859–1899.

Wang, H. L., Fu, C. M., Gopalan, A., & Wen, T. C. (2004). Frequency dependent conductivity of the thin film blend of electroluminescent poly (*p*-phenylene vinylene) with waterborne polyurethane as ionomer. *Thin Solid Films, 466*, 197–203.

Yamamoto, K., & Namikawa, H. (1988). Conduction current relaxation in inhomogeneous conductors. *Japanese Journal of Applied Physics, 27*, 1845–1851.